INTERNATIONAL JOURNAL OF
ADVANCED SCIENTIFIC RESEARCH AND INNOVATION

ISSN: 2785-9541 VOLUME 5, ISSUE 1, 2022, 54 – 66. www.egyptfuture.org/ojs/

Numerical investigation on seismic behavior of steel frame equipped with steel plate shear wall

Hamza Basri[1], Abdelouahab Ras, Karin Hamdaoui, Almoutaz Bellah Alsamawi

[1] EOLE Research Laboratory, Department of Civil Engineering, Faculty of Technology, University of Tlemcen, Tlemcen, Algeria

Abstract

Steel plate shear walls (SPSW) are considered one of the most common and acceptable lateral resisting structural systems for steel structures due to their excellent seismic performance. This system offers several advantages over the other usual lateral load resisting systems such as the conventional braces. Steel saving, installation easiness, reduced foundation cost, and providing major stiffness against building drift are some apparent advantages of the steel plate shear walls. This paper describes and investigates the effect of using steel plate shear walls on the behavior of steel frames. Therefore, finite element (FE) analysis was adopted using ABAQUS software to simulate two steel frames equipped with a steel plate shear wall and conventional brace under cyclic loads. Eigenvalue buckling analysis was conducted as a preliminary analysis and the results were introduced to define the initial imperfection for a realistic simulation. The important seismic parameters including the lateral stiffness, the ultimate shear capacity, energy dissipation, and ductility are investigated using static nonlinear analysis after confirming a good agreement with the results of nonlinear dynamic analysis of the laboratory sample. The numerical results indicated that using SPSW as lateral-load resisting gives higher stiffness, ultimate strength, higher ductility and energy absorption than the conventional brace frame.

Keywords: Steel plate shear wall, Cyclic loading, Numerical simulation, Energy absorption.

ISSN: 2785-9541 VOLUME 5, ISSUE 1, 2022, 54 – 66. www.egyptfuture.org/ojs/

1Introduction

Steel plate shear walls (SPSW) increased in popularity in many countries because of their efficiency and capability against earthquake excitations. Recently it is observed that the SPSW have been demonstrated by many experimental and analytical methods as an effective and economic lateral-load resisting system. These walls improved the energy absorption capacity, superior ductility, high initial stiffness, and stable hysteretic loops. The significant advantages make their usage more effective in strengthening building structures as well as upgrading the old building also. Many types of research have been developed on the topics of the structural response of steel shear walls under static and seismic loadings. The experimental studies on the thin steel shear walls have been conducted under cyclic loading (Berman, 2011). The behavior of trapezoidal corrugated steel plate shear walls was examined by(Farzampour & Laman, 2015), using stiffeners or relatively thick infill plate to avoid the infill plate buckling (Ozcelik & Clayton, 2018). However, this method was non-economical. The thin unstiffened SPSW system was recognized as a successful system against lateral loading, by introducing post-buckling behavior in plates under shear loading. The post-buckling behavior in the thin steel plate shear wall created some problems by the development of tension field action and transmission of excessive stress to the boundary frame. Therefore, huge columns are needed as a solution for this situation and that makes a dilemma (Jiang et al., 2017). To overcome this dilemma some ideas have presented by some researchers as the use of horizontal strut (Phillips & Eatherton, 2018), using concrete to cover the infill steel plate (Wang et al., 2019) and covering the infill plate by Fiber Reinforced Polymer (Sahebjam & Showkati, 2016). One of the reasons for reducing the energy absorption capacity in thin steel plate shear walls without stiffeners is the shear buckling of steel plates under low shear forces.

ISSN: 2785-9541 VOLUME 5, ISSUE 1, 2022, 54 – 66. www.egyptfuture.org/ojs/

The energy absorption capacity in unstiffened steel shear walls is low due to premature buckling (Jebelli & Mofid, 2014), it is confirmed that the value of this out-of-plane buckling is important. The steel plate shear wall systems can be used as stiffened, unstiffened, or using reinforced concrete panels. In SPSW without stiffener, the infill steel plate buckled in compression because of the infill plate's small thickness. Therefore, the lateral forces are resisted by developing tension filed action. This behavior is similar to the plate girders (Valizadeh et al., 2012). While the SPSW with stiffeners has been improving the increase in the buckling capacity of the infill steel plate. Both SPSW and CSPSW provide higher stiffness and shear strength (Shafaei et al., 2017, A),(Shafaei et al., 2018, B)

In this study, the nonlinear response of a steel frame equipped with a steel plate shear wall and the conventional brace is numerically investigated using the finite element ABAQUS program. The seismic characteristics, shear capacity, ductility, energy dissipation, and stiffness degradation of the shear wall and the conventional brace are evaluated and compared.

2Numerical modelling

The numerical study was conducted on a one-story one-bay steel frame using steel plate shear wall and conventional brace, both models were modeled by finite element analysis ABAQUS software.

2.1 Model geometry and finite element properties

The basic geometry for this investigation was a signal-bay one-story steel frame. The bay width was 1410 mm and the story height was 1230 mm. The model consists of a steel plate and its surrounding frame (columns and top beam). The width, height, and thickness of the steel plate were 1410, 960, 2mm respectively. Additionally, four small stiffeners were fixed to the four corners of the steel plate in order to prevent the plate zipping effect. The conventional brace was defined as UPN40.

INTERNATIONAL JOURNAL OF
ADVANCED SCIENTIFIC RESEARCH AND INNOVATION
ISSN: 2785-9541 VOLUME 5, ISSUE 1, 2022, 54 – 66. www.egyptfuture.org/ojs/

All parts of the model components were modeled using the S4R shell element, this element has four nodes and six degrees of freedom for each node. This element is well suited with large displacement and strains, geometric and materials nonlinearities. Figure 1 shows the finite element model of the two cases (SPSW and CBF) and their geometric features are listed in Table 1.

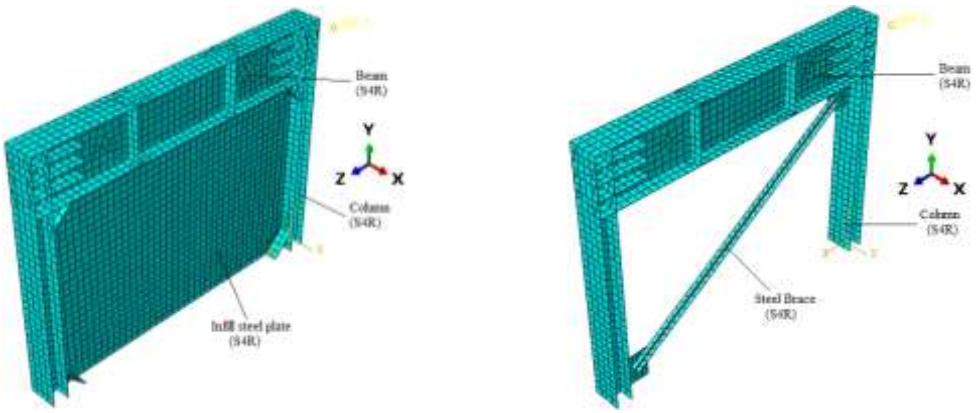

Figure 1: A typical finite element of SPSW and CBF models.

Story height (mm)	Span (mm)	Column section (mm)	Beam section (mm)	Brace section (mm)
1230	1410	H140 x 90 x 20 x 15	140 x 290 x 20 x 20	40 x 20 x 5.5 x 4

Table 1: Geometric specification for the frame members.

2.2 Materials properties

All the steel components have been modeled using elastic-plastic materials in order to evaluate the plastic behavior under the effect of cyclic loading. Materials used for the elements section were low strength steel for the steel plate wall, whereas the material of the other elements was of high strength steel. The yield and ultimate stresses are shown in table 2. The young's modulus and poison's ratio were taken as 200 GPa and 0,3, respectively for the two model frames.

Section	Yielding stress (MPa)	Ultimate stress (MPa)
Steel Plate	192,4	277,2
Beam and Column	414,9	551,8
Brace	258,3	390,4

Table 2: Mechanical properties of steel.

INTERNATIONAL JOURNAL OF
ADVANCED SCIENTIFIC RESEARCH AND INNOVATION
ISSN: 2785-9541 VOLUME 5, ISSUE 1, 2022, 54 – 66. www.egyptfuture.org/ojs/

2.3 Boundary Conditions and loading protocol

The frame is considered as fixed at the ground such that the translation and rotational degree of freedom at the bottom is constrained. Furthermore, out-of-plane displacements of the frame were restrained. For proper performance of the frame, beam to column connections were strengthened by using vertical and horizontal stiffeners at the top beam and beam-column intersection. Both frames are subjected to cyclic lateral loading, applied to the top beam-column junction of the steel frame. The protocol loading according to ATC-24 was selected as shown in Figure 2. The loading pattern consisted of 27 cycles.

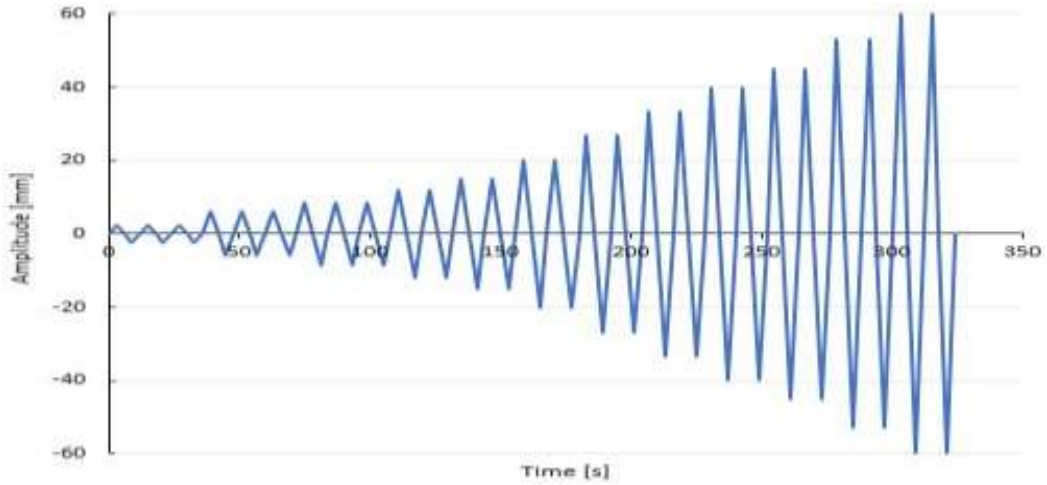

Figure 2: Loading Protocol.

2.4 Buckling analysis

Before doing the nonlinear cyclic analysis, a buckling analysis was conducted to obtain the buckling modes of the plate shear wall, the finite element model of SPSW was subjected to eigenvalue buckling analysis. It should be mentioned that the infill steel plate was effectively used to introduce the initial imperfections in order to allow the numerical model to trigger the deformations. Figure 3 represents the first two buckling modes of the infill steel plate of the web.

INTERNATIONAL JOURNAL OF
ADVANCED SCIENTIFIC RESEARCH AND INNOVATION
ISSN: 2785-9541 VOLUME 5, ISSUE 1, 2022, 54 – 66. www.egyptfuture.org/ojs/

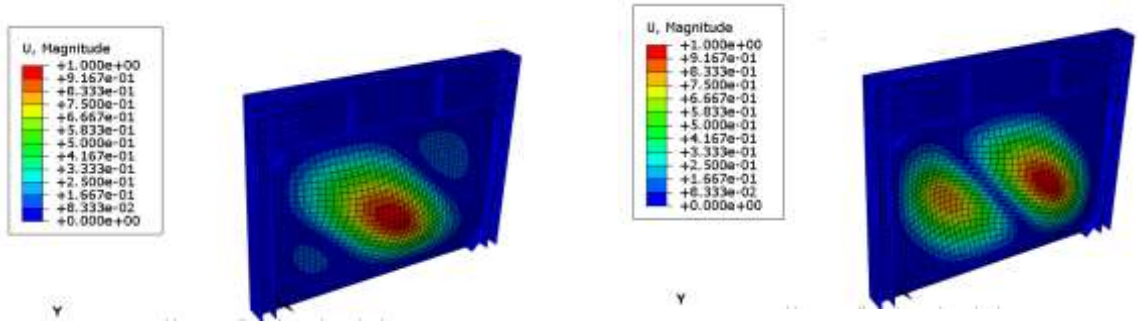

Figure 3: Buckling analysis of steel plate shear wall.

2.5 Verification of finite element method

The results of the present numerical study were verified and well agreed with the experimental results reported by (Sabouri-Ghomi & Sajjadi, 2012). In fact, the SPSW without stiffeners 'DS-PSW' specimen was selected and modeled for this study. Figure 4 shows the comparison between the numerical and the experimental results. As can be seen in the figure, the behavioral hysteresis curves in both the software and the laboratory are very close in each case and have a good fit.

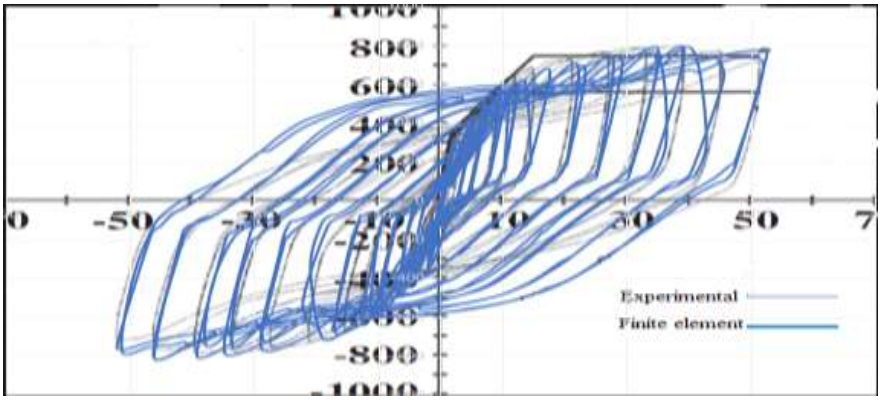

Figure 4: Comparison of Hysteresis Curves of the Numerical model and Laboratory Sample.

3 Results and discussions

3.1 Hysteresis curve

Plots of hysteresis loops for the applied lateral load and displacement of both models are illustrated in Figure 5 and Figure 6. In the model with conventional brace there was no significant yielding happened in the first cycles of loading and the lateral shear load increased gradually.

INTERNATIONAL JOURNAL OF
ADVANCED SCIENTIFIC RESEARCH AND INNOVATION
ISSN: 2785-9541 VOLUME 5, ISSUE 1, 2022, 54 – 66. www.egyptfuture.org/ojs/

The maximum load of the CBF was 480 KN at the story shear displacement of 51,32 mm (5,34% drift) after the buckling of the brace due to the effect of the compressive forces. As seen in Figure 6, the model with SPWS shows the elastic behavior during the first five cycles. After the yielding point, the behavior changed to the plastic region with a maximum load of 776,7 KN at the story shear displacement of 39,08 mm (4,07% drift). The maximum drift of the SPSW frame was 5,46% after the buckling of the steel plate.

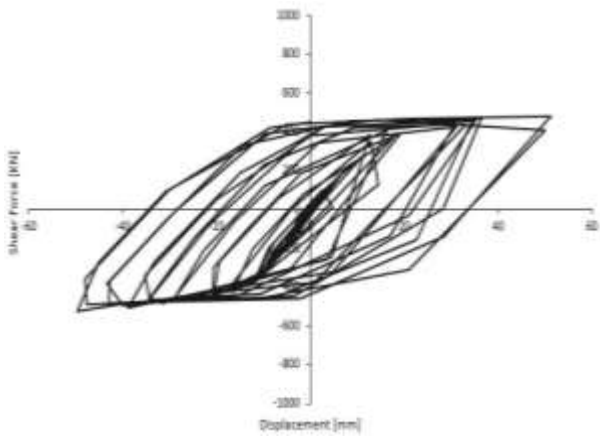

Figure 5: Hysteresis curve of CBF specimen

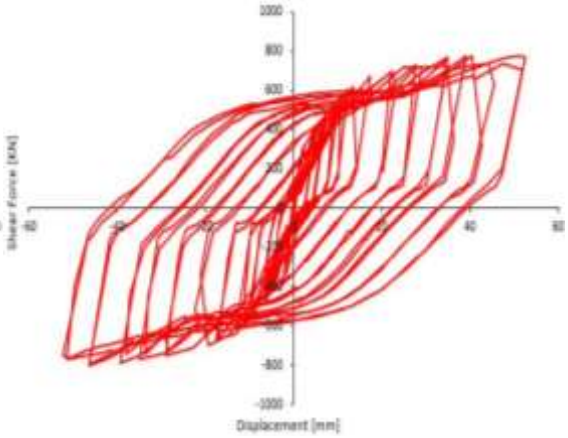

Figure 6: Hysteresis curve of SPSW specimen.

Comparing the hysteresis behavior between the two frames, both models have the same behavior in the elastic region and basically reach the same story shear displacement. The two hysteresis diagrams show a difference between the two systems. The SPSW model shows more shear forces capacity and wide hysteresis loops compare with the frame with CB and that indicates the greatly improved behavior of energy dissipation and ductility of SPSW system. Moreover, the curving cycles in the SPSW frame became more stable, uniform and symmetric compare with those of the CBF model.

INTERNATIONAL JOURNAL OF
ADVANCED SCIENTIFIC RESEARCH AND INNOVATION
ISSN: 2785-9541 VOLUME 5, ISSUE 1, 2022, 54 – 66. www.egyptfuture.org/ojs/

3.2 Skeleton curve and ductility

From Figure 7 the overall skeleton curve of the two frames shows the seismic performance difference of (SPSW and CBF), and it can be easily recognized the good load carrying capacity of SPSW against the conventional brace. Furthermore, it can divide the whole loading process of the skeleton curve into three regions (Elastic, elastic-plastic, and failure). As summarized in Table 3, the yield point, maximum loads, and displacement are determined from the skeleton curve using the graphical method as shown in Figure 8.

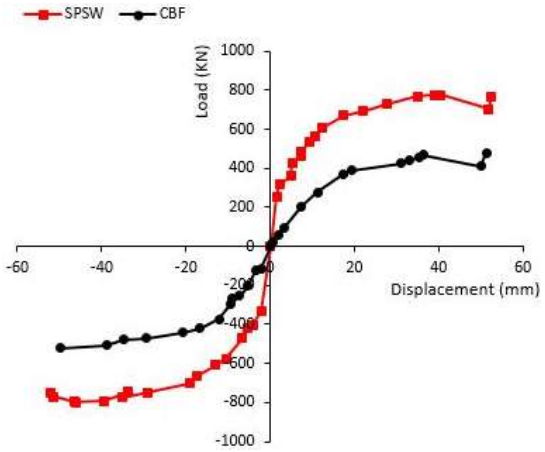

Figure 7: Skeleton Curve of SPSW and CBF.

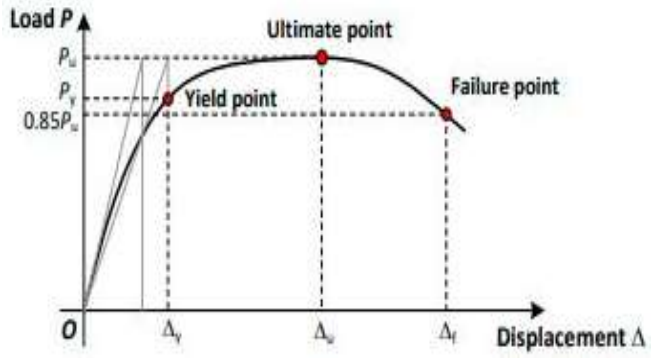

Figure 8: Characteristic points on load-displacement curve.

Ductility is an important parameter in the evaluation of the cyclic behavior of frames, it was calculated as the ratio of maximum displacement Δ_{max} to the yield displacement $\Delta_{y.}$

INTERNATIONAL JOURNAL OF
ADVANCED SCIENTIFIC RESEARCH AND INNOVATION
ISSN: 2785-9541 VOLUME 5, ISSUE 1, 2022, 54 – 66. www.egyptfuture.org/ojs/

The displacement ductility coefficients μ values in both loading directions are listed in Table 3. The displacement ductility of SPSW reached as much as 7,21, which is considerably greater than the value of 4,57 for the CBF. This high ductility capacity represents one of the advantages of using shear walls with low-yield steel plates.

Maximum load							Maximum displacement					
	Positive loading (+)			Negative loading (-)			Positive loading (+)			Negative loading (-)		
Specimen	P_{max} (KN)	Δ (mm)	Story drift (%)	P_{max} (KN)	Δ (mm)	Story drift (%)	P (KN)	Δ_{max} (mm)	Story drift (%)	P (KN)	Δ_{max} (mm)	Story drift (%)
SPSW	776,7	39,08	4,07	-800,61	-46,23	4,82	768,4	52,46	5,46	-751,6	-52,26	5,44
CBF	480	51,32	5,34	-521,2	-49,7	5,17	480	51,32	5,34	-521,2	-49,7	5,17
Yield point												
	Positive loading (+)				Negative loading (+)				P_{max}/P_y		Δ_{max}/Δ_y (Disp -Ductility)	
Specimen	P_y (KN)	Δ_y (mm)	Story drift (%)	K_y (KN/mm)	P_y (KN)	Δ_y (mm)	Story drift (%)	K_y (KN/ mm)	Positive loading	Negative loading	Positive loading	Negative loading
SPSW	461,2	7,27	0,75	63,44	-472,3	-6,64	0,7	71,1	1,68	1,69	7,21	7,8
CBF	277,3	11,22	1,16	24,71	-292,1	-9,33	0,97	31,3	1,73	1,78	4,57	5,32

Table 3: Summary of Numerical results.

3.3 Energy Absorption

For evaluating the energy absorption capacity of the finite element models, it can be computed from the force-displacement hysteresis loops as shown in Figure 9. The accumulated energy dissipation of the two models is illustrated in Figure 10. As can be seen, the energy absorption is low and almost the same for the two system frames at the first fourth loading stages. After that, the energy consumption capacity of the SPSW frame increases more rapidly than that of the CBF. At the end of loading the energy dissipated by the shear wall reached 372,12 KN.m at a maximum drift of 5,46% greater than 196,8 KN.m at a maximum drift of 5,34% of the CBF, and this is explained by the uniform plastic deformation distributed along with the steel plate height which improved the ability of the shear wall to sustain large deformation under cyclic loads.

INTERNATIONAL JOURNAL OF
ADVANCED SCIENTIFIC RESEARCH AND INNOVATION
ISSN: 2785-9541 VOLUME 5, ISSUE 1, 2022, 54 – 66. www.egyptfuture.org/ojs/

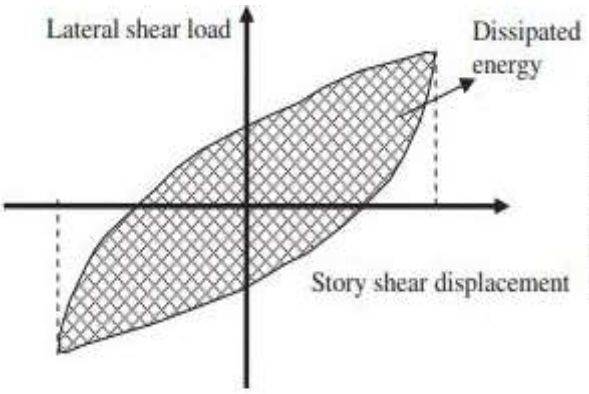

Figure 9: Energy dissipation capacity calculation diagram.

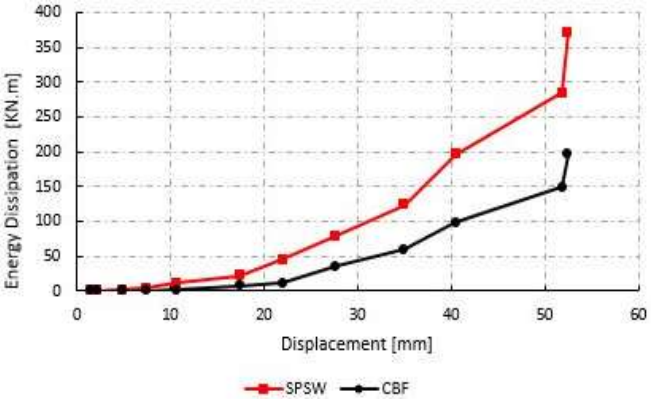

Figure 10: Energy dissipation capacity.

3.4 Stiffness degradation

Figure 11 describes the stiffness degradation of both SPSW and CBF frames. The secant stiffness K_i is calculated for each loading cycle and is expressed by the ratio between the maximum load P_{max} at cycle i and the corresponding maximum displacement Δ_i at cycle i. From Figure 11 it can be seen clearly that the initial stiffness of SPSW is greater than the CBF. It can be found that the stiffness of both frames decreases obviously with the increase of displacement until reached the top story drift of 5,46% which makes the final residual stiffness 14,76 KN/mm and 9,35 KN/mm for the SPSW and CBF frames respectively.

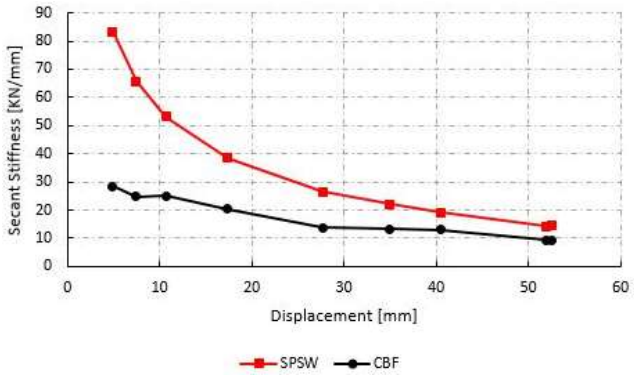

Figure 11: Stiffness degradation of SPSW and CBF.

ISSN: 2785-9541 VOLUME 5, ISSUE 1, 2022, 54 – 66. www.egyptfuture.org/ojs/

4 Conclusion

A numerical study was performed to investigate the potential maximum ductility, energy absorption and stiffness degradation of two frames equipped by SPSW and CB. The two frames were modeled and analyzed using the finite element program ABAQUS. For verification of the modeling, an experimental laboratory sample result was compared and confirmed with the numerical study by using nonlinear static analyses. The simulation results improved the use of steel plate shear wall as a lateral-load resisting system compared with the traditional brace. Based on the numerical analysis, the hysteresis curve of force-shear displacement of the SPSW frame was more symmetric and stable in shape than the hysteresis curve of the CBF, this behavior demonstrates the excellent deformation capacity of steel plates. The yielding and maximum loads of steel plate shear wall were 1,66 times and 1,62 times of CBF respectively. The respective values of displacement ductility of SPSW in both directions were 1,58 times and 1,47 times those of CBF respectively. The area of total hysteresis loops of SPSW was 1,9 times of CBF. Moreover, the elastic lateral stiffness of the SPSW was 2,6 times those of the CBF. From the above results, it is observed that using steel plate shear walls led to increasing the lateral strength and ductility. Therefore, it creates symmetry in the resistance of the steel plate during the loading process in both directions (tension and compression). Hence, it increased the ability of the shear walls to withstand a large amount of seismic energy compared with the traditional braces.

ISSN: 2785-9541 VOLUME 5, ISSUE 1, 2022, 54 – 66. www.egyptfuture.org/ojs/

References

1. Applied Technology Council. Guidelines for Cyclic Seismic Testing of Components of Steel Structures; 1992. ATC-24, Redwood City, CA.
2. Berman, J. W. (2011). Seismic behavior of code designed steel plate shear walls. Engineering Structures, 33(1), 230–244. https://doi.org/10.1016/j.engstruct.2010.10.015
3. Farzampour, A., & Laman, J. A. (2015). Behavior prediction of corrugated steel plate shear walls with openings. Journal of Constructional Steel Research, 114, 258–268. https://doi.org/10.1016/j.jcsr.2015.07.018
4. Jebelli, H., & Mofid, M. (2014). Effects of using low yield point steel in steel plate shear walls. IES Journal Part A: Civil and Structural Engineering, 7(1), 51–56. https://doi.org/10.1080/19373260.2013.858646
5. Jiang, L., Zheng, H., & Hu, Y. (2017). Experimental seismic performance of steel- and composite steel-panel wall strengthened steel frames. Archives of Civil and Mechanical Engineering, 17(3), 520–534. https://doi.org/10.1016/j.acme.2016.11.007
6. Ozcelik, Y., & Clayton, P. M. (2018). Behavior of columns of steel plate shear walls with beam-connected web plates. Engineering Structures, 172(January), 820–832. https://doi.org/10.1016/j.engstruct.2018.06.087
7. Phillips, A. R., & Eatherton, M. R. (2018). Computational study of elastic and inelastic ring shaped – steel plate shear wall behavior. Engineering Structures, 177(September), 655–667. https://doi.org/10.1016/j.engstruct.2018.10.008
8. Sabouri-Ghomi, S., & Sajjadi, S. R. A. (2012). Experimental and theoretical studies of steel shear walls with and without stiffeners. Journal of Constructional Steel Research, 75, 152–159. https://doi.org/10.1016/j.jcsr.2012.03.018

ISSN: 2785-9541 VOLUME 5, ISSUE 1, 2022, 54 – 66. www.egyptfuture.org/ojs/

9. Sahebjam, A., & Showkati, H. (2016). Experimental study on the cyclic behavior of perforated CFRP strengthened steel shear walls. Archives of Civil and Mechanical Engineering, 16(3), 365–379. https://doi.org/10.1016/j.acme.2016.01.009
10. Shafaei, S., Farahbod, F., & Ayazi, A. (2017). Concrete Stiffened Steel Plate Shear Walls With an Unstiffened Opening. Structures, 12, 40–53. https://doi.org/10.1016/j.istruc.2017.07.004
11. Shafaei, S., Farahbod, F., & Ayazi, A. (2018). The wall–frame and the steel–concrete interactions in composite shear walls. Structural Design of Tall and Special Buildings, 27(11), 1–16. https://doi.org/10.1002/tal.1476
12. Valizadeh, H., Sheidaii, M., & Showkati, H. (2012). Experimental investigation on cyclic behavior of perforated steel plate shear walls. Journal of Constructional Steel Research, 70, 308–316. https://doi.org/10.1016/j.jcsr.2011.09.016
13. Wang, J., Wang, F., Shen, Q., & Yu, B. (2019). Seismic response evaluation and design of CTSTT shear walls with openings. Journal of Constructional Steel Research, 153, 550–566. https://doi.org/10.1016/j.jcsr.2018.11.002